Journal of Civil and Environmental Engineering Vol. 53 (2023), No. 2 (Summer), 168-179

University of Tabriz

Journal of Civil and Environmental Engineering

# Numerical Analysis of Plastic Hinge Regions in RC Deep Beams under Concentrated and Distributed Loads

Dina Ghazi-Nader, Reza Aghayari *

*Department of Civil Engineering, Razi University, Kermanshah, Iran*

Received 5 September 2020, Received in revised form 24 December 2021, Accepted 17 January 2022

**ABSTRACT:**

Plastic hinge properties play a crucial role in predicting the nonlinear response of structural elements. The plastic hinge region of reinforced concrete normal beams has been previously studied experimentally and analytically. The main objective of this research is to evaluate the behavior of the plastic hinge region of reinforced concrete deep beams and its comparison with normal beams through finite element simulation. To do so, ten beams contain six deep beams, and four normal beams, under concentrated and uniformly distributed loading, are investigated. Lengths in the plastic hinge region involving curvature localization, rebar yielding, and concrete crushing zones are studied. The results indicate that the curvature localization zone is not suitable for the prediction of plastic hinge length in reinforced concrete deep beams. Based on the results it can be stated that in simply supported normal beams the concrete crushing zone is focused on the middle span, but in simply supported deep beams by creating a compression strut between loading place and support, the concrete crushing zone spreads along the compression trajectory. The rebar yielding zone of simply supported beams increases as the loading type is changed from the concentrated load at the middle to the uniformly distributed load.

**KEYWORDS:**

Plastic hinge; RC deep beam; Nonlinear strain; Reinforced concrete; Finite element analysis

## 1. Introduction

The plastic deformation of reinforced concrete (RC) members which is defined as the ability of members to develop their flexural strength and ultimate load-carrying before failure has been a subject of interest in RC structural researchers. Plastic hinge zone, in which plastic deformation of the member is concentrated in that, absorbs energy and prevents structural collapse during seismic events. The Physical plastic hinge zone of structures is a zone that is damaged by the forces and efforts, in reinforced concrete structures slippage and yielding of rebar, and crushing of concrete is created. In addition to designing new structures, the reconstruction of old structures requires the quantification of the plastic hinge zone. For example, it is important to know the extent of rebar slipping zone and area of concrete crushing for retrofitting work by FRP (Fiber Reinforced Polymer) jacketing. The length of the plastic hinge depends on many parameters including material properties of the concrete and rebar, reinforcement ratio, cover of concrete, loading scheme, dimensions of the member, and so on. Hence the determination of the length of plastic hinges is difficult. Due to the complexity involved, most studies of the plastic hinge in RC members have been done by experimental testing. Some well-known equations for estimating the plastic hinge length ($L_p$) are summarized in Table1. None of these models have contained all the influential factors (Zhao et al., 2012).

A laboratory experiment is restricted by the cost and time and on the other hand, increasing the power and speed of computers has made numerical modeling easier. Therefore, the finite element method has found wide applications in analyzing structures in recent years.

* Corresponding Author

*E-mail addresses:* dina.ghazinader@gmail.com (Dina Ghazi-Nader), reza_agh@razi.ac.ir (Reza Aghayari).

**Table 1.** Empirical models for plastic hinge length

| Researcher Reference | Plastic hinge length ($L_p$) |
|---|---|
| Baker (Baker, 1956) | $k(z/d)^{1/4}d$ (for RC beams and columns) |
| Sawyer (Sawyer, 1965) | $0.25d + 0.075z$ |
| Corley (Corley, 1966) | $0.5d + 0.2\sqrt{d}(z/d)$ (for RC beams) |
| Mattock (Mattock, 1967) | 0.5d+0.05z (for RC beams) |
| Paulay and Priestley (Paulay and Priestley, 1992) | $0.08z + 0.022d_b f_y$ (for RC beams and columns) |
| Coleman and Spacone (Coleman and Spacone, 2001) | $G_f^c/\left[0.6f'_c(\varepsilon_{20} - \varepsilon_c + 0.8f'_c/E_c)\right]$ |
| Panagiotakos and Fardis (Panagiotakos and Fardis, 2001) | $0.18z + 0.021d_b f_y$ (for RC beams and columns) |
| Bohl and Adebar (Panagiotakos and Fardis, 2001) | $(0.2l_w + 0.05h_w)\left(1 - 1.5P/f'_c A_g\right) < 0.8l_w$ (for RC wall) |
| Wallace (Panagiotakos and Fardis, 2001) | $0.33l_w$ (for RC wall) |
| Yuan and Wu (Panagiotakos and Fardis, 2001) | $0.18L + 0.021d_b f_y$ (for columns) |
| FEMA 356 (Panagiotakos and Fardis, 2001) | 0.5d (for RC beams and columns) |

k: curvature, z: distance from critical section to point of contraflexure, d: effective depth of beam or column
db: diameter of longitudinal reinforcement, fy: yield strength of reinforcement, fc: concrete compressive strength
$G_f^c$: concrete fracture energy in compression, $E_c$: Young's modulus of concrete, $\varepsilon_c$: concrete compressive strain
$\varepsilon_{20}$: strain at which the stress reaches 20% of fc after peak stress, $l_w$:length of wall, $h_w$: height of wall, $A_g$: wall cross_section area, $P$: axial load

Zhao et al. (Zhao et al., 2011) analyzed the plastic hinge of reinforced concrete normal beams. The extent of the rebar yielding zone, concrete crushing zone, curvature localization zone, and the real plastic hinge length were studied using the finite element method. The results showed that none of the existing empirical models are adequate for the prediction of the plastic hinge length. Parametric studies were subsequently employed to investigate the plastic hinge length in terms of dimensions of the member, material properties of rebar and concrete, and reinforcement ratio. Kheyroddin et al. (KHEYR and Naderpour, 2007) conducted a parametric study by finite element method to assess the influence of the tension reinforcement index, and the loading type on the ultimate deformation characteristics of reinforced concrete beams. Based on the analytical results, a new simple equation as a function of the tension reinforcement index and the loading type was proposed. Based on the test results conducted by Lopez et al. (López et al., 2020), the shear strength provided by concrete was studied concerning the bending rotation and the average crack width in reinforced concrete beams with shear reinforcement. It was confirmed that increasing bending rotations and crack widths decrease the shear strength of concrete. Pokhrel et al. (Pokhrel and Bandelt, 2019) presented a finite element model to study the plastic hinge region behavior of high-performance fiber-reinforced cementitious composites flexural members with variations in mechanical properties, boundary conditions, and geometric properties. A mechanical interpretation of the different mechanisms contributing to the damage localization at the plastic hinge region was provided by Pereira and Romao (Pereira and Romão, 2020). Urthermore, an experimental database of damage length in RC frame components compiled from the technical literature was compiled from the technical literature and used to assess the adequacy of each of the mechanisms to model the observed damage patterns. In Schlappal et al. (Schlappal et al., 2020) work, analytical formulae, expressing maximum tolerable relative rotations as a function of the normal force transmitted across reinforced concrete hinges was derived. The usefulness of the derived formulae was assessed by means of experimental data taken from the literature.

RC deep beams are vital structural members carrying heavy loads over a short span, that are used in high-rise buildings, bridges, dams, offshore piers, and shear walls. The ACI Building code (Code, 2014) defines deep beams as members having either: clear spans equal to or less than four times the overall member depth; or regions with concentrated loads in the range of twice the member depth from the surface of the support. In these beams, the ratio of the height to the span is larger than the standard limit and the thickness of the beam is low compared to its height. Due to the geometry of deep beams, they behave as two-dimensional members. The plane sections do not remain plane in bending, as a result, the bending elementary concept for normal beams may not be appropriate and Euler Bernoulli's theory does not apply to deep beams (Niranjan and Patil, 2012). The shear strength of a deep beam is affected by many factors such as shear span-to-depth ratio, concrete compressive strength, longitudinal reinforcement, web reinforcement, beam depth, beam span-to-depth ratio, loading and supporting conditions, and type of concrete. However, the shear span-to-depth ratio is the most significant factor that affects the shear strength of a deep beam (Adinkrah-Appiah and Adom-Asamoah, 2016). There are plenty of researches that have investigated various subjects related to deep beams. Observed by Arabzadeh et al. (Arabzadeh et al., 2011) that the horizontal shear reinforcement is most effective when aligned perpendicular to the major axis of diagonal crack. Aguilar et al.(Aguilar et al., 2002)proposed that the provision of shear

reinforcement within the middle region of the shear span can improve the ultimate shear strength of deep beams. In Mohamed et al. (Mohamed et al., 2014a) work, a reduction in the beam capacity was observed when tension reinforcement distribution depth was increased and it was suggested that the reinforcement distribution should be in the range of 0.1 H -0.2H for simply supported deep beams. Yang et al. (2003) concluded that the effect of concrete strength on the nominal shear strength appears more significant in deep beams than in normal beams because most loads are transferred by concrete struts. Wang et al. (Wang and Meng, 2008) presented a new modified model for predicting the shear strength of concrete deep beams. This model was designed for predetermined simple structure beams. An experimental and theoretical program consisting of nine concrete deep beams specimens was carried out by Hussein et al.(2018) to investigate the effect of loading and supporting area on the shear strength of concrete deep beams. The research evidence provided that by proper configuration of loading and supporting areas, the shear strength of concrete deep beams can be increased. Ibrahim et al. (2018) developed a parametric study using both of ABAQUS program and specifications of the ACI 318-14 to investigate the relationship between the shear strength of deep beams with different sizes of shear openings and shear opening ratio to the total area of the shear zone. Based on this parametric study, a dimensionless equation for calculating the shear strength of deep beams having the same shear span-to-depth ratio was obtained. Demir et al. (2019) reported that the load-carrying capacity of the RC deep beams increases with an increase in section height, the shear strength of the deep beams increases with a decrease in the ratio of shear span to effective depth. Also, they reported that crack widths increment as section height increases. Chen et al. (2018) proposed a novel cracking strut-and-tie model (CSTM) to better predict the shear strength of a deep beam. The results show that the prediction of the proposed model is better than those of other models and can describe well the influences of main design parameters such as shear span to depth ratio, longitudinal bar ratio, web reinforcement ratio, concrete compressive strength, and effective depth on the shear resistance of deep beams. Ma et al. (Ma et al., 2022) analyzed influences of factors including reinforcement ratio, shear span-to-depth ratio, depth-to-width ratio, and compressive strength of concrete on the shear behavior of the reinforced concrete deep beams. It was found that the shear strength of deep beams decreases with an increase of the shear span-to-depth ratio and the concrete strength, depth-to-width ratio, and web reinforcement ratio parameters affect significantly this trend. Furthermore, an equation for the ultimate shear strength of deep beams corresponding to the minimum sectional size was also suggested.

Due to the high complexity of the behaviour of plastic hinge of reinforced concrete members, very limited knowledge has been obtained and there is no definitive theoretical formulation to calculate plastic hinge length. The behaviour of deep beams, which is different from simple beams, adds to this complexity. There is no information on the study of plastic hinge region in RC deep beams in the literature. In the previous work, we briefly investigated the rebar yielding zone and concrete crushing zone methods for estimating the length of a plastic hinge, in the case of deep beam (Ghazi-Nader and Aghayari, 2018). This study aims to investigate the plastic hinge region of RC deep beams and compare it with normal beams through finite element (FE) numerical simulations via ABAQUS software. First, the numerical modeling has been verified by comparing the numerical results to experimental work in the literature. Then the plastic hinge region involving curvature localization zone, rebar yielding zone, and concrete crushing zone has been investigated.

## 2. Numerical Modeling and Validation

A large number of commercial finite element software have shown adequate reliability and accuracy to study the behavior of reinforced concrete structures. In the present study, the Finite Element simulation software ABAQUS which can solve a wide range of linear and nonlinear problems, was employed. The concrete damaged plasticity (CDP) model, which provides the capability of modeling concrete and other quasi-brittle materials, was used for defining the inelastic behavior of concrete. This model considers the isotropic damaged elasticity concept with isotropic tensile and compressive plasticity. It assumes that tensile cracking and compressive crushing of the concrete material are the main two failure mechanisms. The CDP parameters considered in the FE model were assumed as follows: dilation angle $\psi$=56 degrees, eccentricity $\epsilon$=0.1. The ratio of maximum compressive stresses in biaxial to maximal stresses in the uniaxial state (fb0/fc0) was 1.16 and the ratio of the second stress invariant on the tensile meridian ($K$) was 0.667. To use the visco-plastic properties of concrete in the model, a viscosity coefficient of 0.0001 s was input. More detailed information related to CDP parameters can be found in the ABAQUS user's manual (Manual, 2008). Uniaxial compressive and tensile constitutive material behaviors of concrete are required to define the CDP model. Typical compressive and tensile stress-strain relationships in ABAQUS are illustrated in Fig. 1.

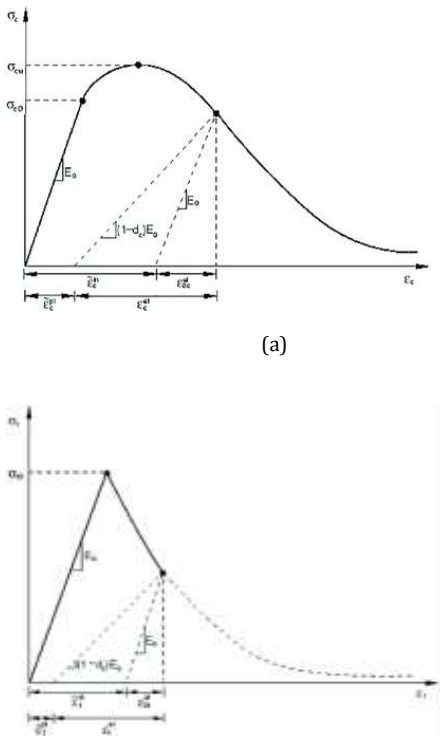

(a)

(b)

**Fig. 1.** The stress-strain curve of concrete in CDP model, (Manual, 2008): (a) Compressive behavior, (b) Tensile behavior

The stress-strain relations under uniaxial compression and tension loading are, respectively (Manual, 2008):

$$\sigma_c = (1 - d_c)E_0\left(\varepsilon_c - \varepsilon_c^{pl}\right) \quad (1)$$

$$\sigma_t = (1 - d_t)E_0\left(\varepsilon_t - \varepsilon_t^{pl}\right) \quad (2)$$

Where E0 is the initial elastic stiffness of the material, $\varepsilon_c^{pl}$ and $\varepsilon_t^{pl}$ are plastic strains for compression and tension respectively, $d_t$ is the tensile damage parameter which automatically converts the cracking strain values to plastic strain values using the following relationship.

$$\varepsilon_t^{pl} = \varepsilon_t^{ck} - \frac{d_t}{(1 - d_t)}\frac{\sigma_t}{E_0} \quad (3)$$

And $d_c$ is compressive damage parameters, it converts the crushing strain values to inelastic strain values as follows.

$$\varepsilon_c^{pl} = \varepsilon_c^{in} - \frac{d_c}{(1 - d_c)}\frac{\sigma_c}{E_0} \quad (4)$$

The cracking strain ($\varepsilon_t^{\sim ck}$) is defined as the total strain ($\varepsilon_t$) minus the elastic strain corresponding to the undamaged material ($\varepsilon_{0t}^{el} = \sigma_t/E_0$). The compressive inelastic strain ($\varepsilon_c^{\sim in}$) is defined as the total strain ($\varepsilon_c$) minus the elastic strain related to the undamaged material ($\varepsilon_{0c}^{el} = \sigma_c/E_0$). According to Fig. 2, a trilinear stress-strain curve is used to define the steel material behavior in the ABAQUS program.

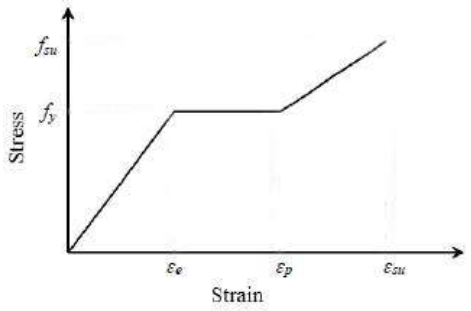


**Fig. 2**. Equivalent stress-strain curve of steel

To validate the finite element model, an experimental specimen (DB 1.0-0.75), studied by Roy and Brena (Roy and Brena, 2008) has been analyzed. The specimen is simply supported deep beam under concentrated load. Fig. 3 shows the geometry, cross-section, and reinforcement details of the beam. The reinforcement consists of main longitudinal reinforcing bars #5 (19mm in diameter) at the bottom and #3 (10mm in diameter) at top of the section with average yield stress equal to 469MPa and 414MPa respectively. Web reinforcement consisting of vertical stirrups and horizontal bars formed using bar D4 wire (corresponding to a diameter of about 5,5mm) with an average measured yield stress equal to 605MPa. The material properties for concrete with 30MPa ultimate compressive strength are derived using the above relationship. Three-dimensional FE Model was used to increase the accuracy of numerical results. The element type used for the concrete beam was an 8-node solid element (C3D8R). Embedded truss reinforcement a 2-node linear 3D truss element (T3D2) was utilized to model steel rebars. Bonding between concrete and rebars was executed by the embedded constraint technique which considers concrete as the host region and bars as an embedded region. To avoid stress concentration at support and loading points, steel plates were added to the model. The load is applied as a vertical displacement on the loading plate. Supports are considered as a pin and a roller as in the test. The general view of the ABAQUS model of reinforcement is depicted in Fig. 4. The size of the mesh is closely related to the accuracy and number of mesh required for the meshing of the element. To determine a more accurate mesh size for the finite element model, a parametric study is performed. As a result, 50mm mesh size with an aspect ratio of 1 is determined as an optimum mesh size. The meshed model is demonstrated in Fig. 5.

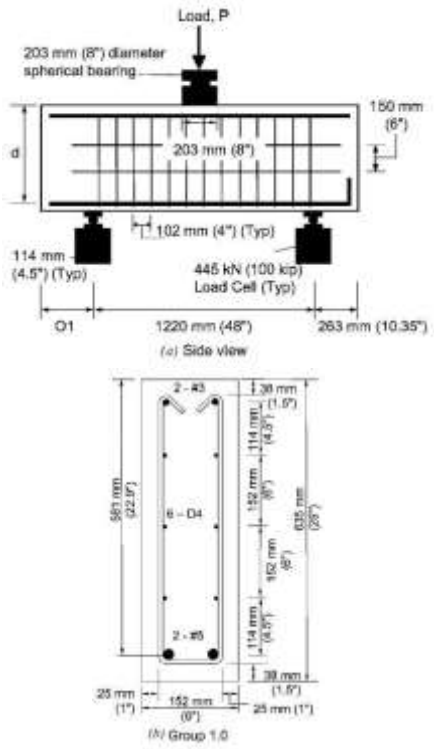


**Fig. 3**. Specimen geometry and cross section, (Roy and Brena, 2008)

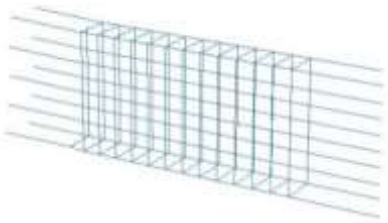

**Fig. 4**. The reinforcement details of beam specimen

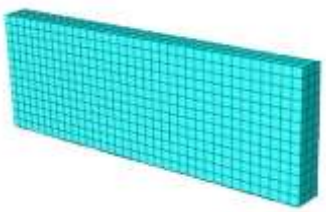

**Fig. 5**. The applied mesh for beam specimen

The load-deflection response of the studied beam is compared with the experimental results in Fig. 6. The numerical result shows a good agreement with the experimental results. As it can be seen on the load-deflection curve, the stiffness of the FE model is higher than that of the test, because FE models do not include micro-cracks and some other ambient factors that may have reduced the stiffness of the tested specimen in real.

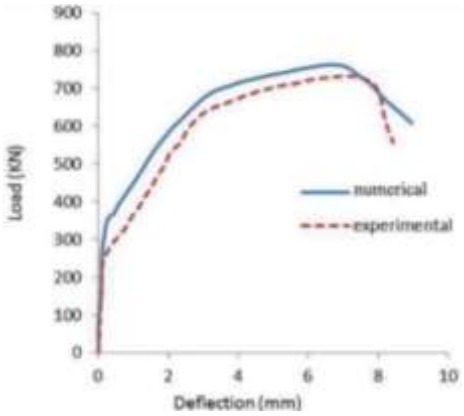


**Fig. 6**. Load-Deflection Curve

## 3. Description of studied beams

Ten beams were investigated in this study. The overall shapes of the beams are depicted in Fig. 7. All beams had a width of 152 mm and a free span length of 1220mm. Different depths were considered to satisfy the desired L/h. ("L" is the free span length of the beam and "h" is the depth of the beam). The values of L/h are 6, 5, 4, 3, and 2. That beams with L/h 4, 3, and 2 are deep. Sufficient horizontal and vertical web reinforcement according to ACI318-14 provisions were used to ensure tensile reinforcement yielding before concrete failure because plastic hinge will be formed in beams with flexural failure mode. According to the code, the use of horizontal shear reinforcement is necessary for deep beams. Therefore, the minimum amount was used. Specifications of modeled beams are presented in Table2.

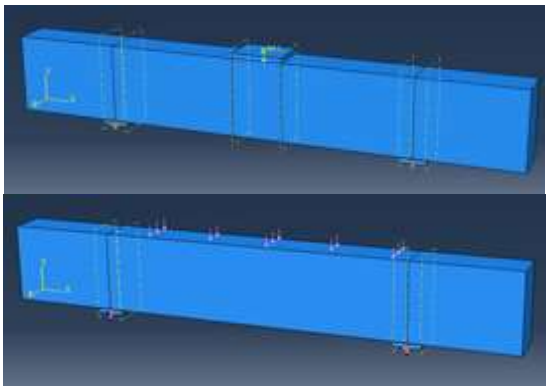

**Fig. 7.** Shape of concrete beams modeled in ABAQUS

**Table 2**. Specifications of modeled beams

| Beam ID | Span-to-Depth ratio (L/h) | Loading Type | Reinforcement | | Stirrup | | $f_c$ (Mpa) | $f_y$ (Mpa) | |
|---|---|---|---|---|---|---|---|---|---|
| | | | Tension | Compression | Vertical | Horizontal | | ϕ10 , ϕ20 | Φ6 |
| B16 | 6 | Concentrated | 2 ϕ20 | 2 ϕ10 | 25 ϕ6@102mm | - | 30 | 400 | 340 |
| B15 | 5 | Concentrated | | | | - | | | |
| B14 | 4 | Concentrated | | | | 6 ϕ6 | | | |
| B13 | 3 | Concentrated | | | | 6 ϕ6 | | | |
| B12 | 2 | Concentrated | | | | 6 ϕ6 | | | |
| B26 | 6 | Distributed | | | | - | | | |
| B25 | 5 | Distributed | | | | - | | | |
| B24 | 4 | Distributed | | | | 6 ϕ6 | | | |
| B23 | 3 | Distributed | | | | 6 ϕ6 | | | |
| B22 | 2 | Distributed | | | | 6 ϕ6 | | | |

## 4. Investigation of plastic hinge regions and results

### *4.1. Curvature*

The plastic hinge length is generally defined as an equivalent length where the curvature is assumed as constant(Park and Paulay, 1991). The equivalent plastic hinge length can be determined by curvature as follows:

$$L_P = \frac{\theta_P}{\emptyset_u - \emptyset_y} \quad (5)$$

Where $\theta_p$ is plastic rotation and it is obtained by integration along the yielding length (where the curvature in the section is higher than its yielding curvature), of difference between the ultimate curvature ($\emptyset_u$), and the yielding curvature ($\emptyset_y$). Average curvature ($\emptyset$) for a certain section of the beam can be calculated using the requirements of strain compatibility and equilibrium of forces as following relationship (Mohamed et al., 2014b).

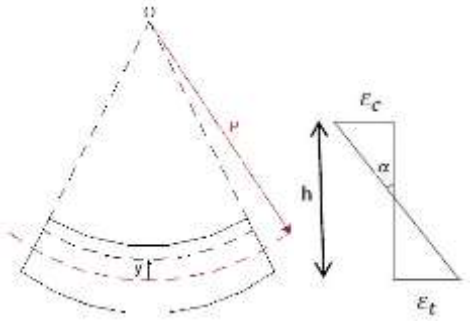


**Fig. 8**. Element of a beam in bending.

$$\emptyset = \frac{|\varepsilon_t| + |\varepsilon_c|}{h} \quad (6)$$

Where $\varepsilon_t$, and $\varepsilon_c$,are strains at the tension and compression ends of the strain profile, respectively. Strain profiles at the mid-span of the studied beams are depicted in Fig. 9. As shown the distribution of strain in deep beams is completely different from the linear ones, commonly accepted for normal beams. Accordingly, the strain distribution of deep beams is non-linear even at the elastic stage. Also, it is found that the smaller the span/depth ratio, the more pronounced the deviation of the strain distribution from that of Euler Bernoulli's theory.

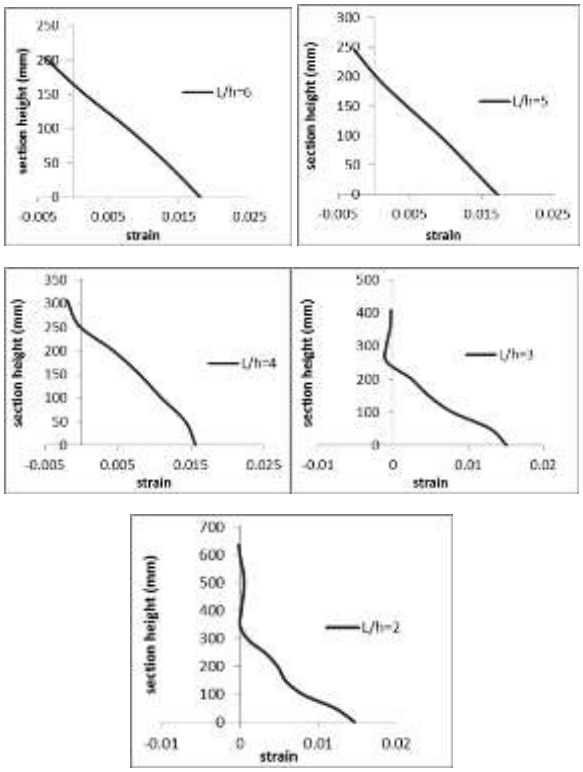


**Fig. 9**. Strain distribution graph in the middle span of simply supported beams under concentrated load

Besides strain distribution graphs for two sections of the deep beam with L/h=2, are compared in Fig. 10. As can be seen, the strain distributions at various sections of a deep beam are different from each other, unlike the normal beam. Thus, due to the non-linear distribution of strain, the curvature is various across the depth of deep beams.

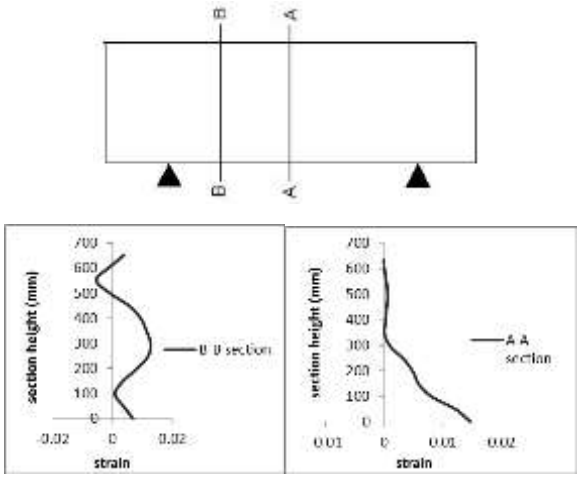


(a) (b)

**Fig. 10**. Strain distribution graph: (a) B-B section, (b) A-A section.

For a more and better explanation, curvature distribution from the support to the mid-span at three different heights of one normal beam and one deep beam are shown in Fig. 11. As can be seen, curvature distribution at different heights of the deep beam does not have the same trend as that in a normal beam. Therefore, it is concluded that the curvature localization zone cannot be suitable for the prediction of plastic hinge length in deep beams.

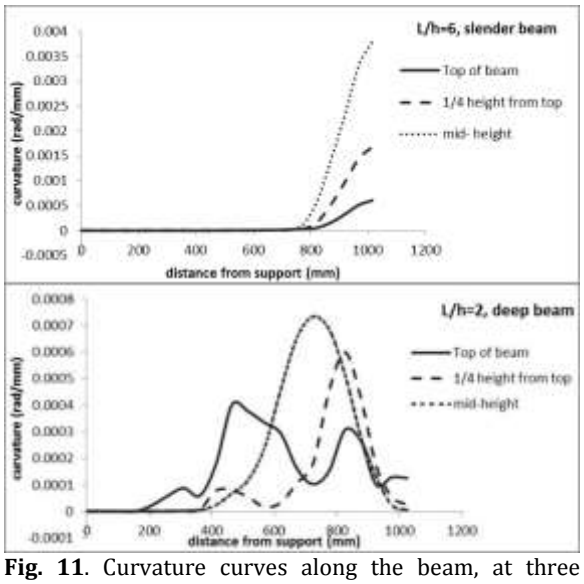


**Fig. 11**. Curvature curves along the beam, at three different heights for normal and deep beam

### *4.2. Rebar yielding zone and Concrete crushing zone*

In addition to curvature, another approach to evaluating the plastic hinge length proposed by some researchers is the length of the rebar yielding zone (Zhao et al., 2011; Elmenshawi et al., 2012).The rebar yielding zone is a zone where reinforcing steel strain in tension is more than $\varepsilon_{sy}$, ($\varepsilon_{sy} = f_y/E_s$). Where $f_y$ is the yield strength of reinforcement and $E_s$ is the young's modulus of reinforcement. The crushing zone of concrete is also considered as plastic hinge region in some researches (Zhao et al., 2011; Legeron and Paultre, 2000; Abdel-Fattah and Wight, 1987). In numerical analysis, the crushing zone can be quantifiable by the compressive strain of concrete. For this purpose, two regions of the beam included the compression region where the concrete strain is more than strain at peak concrete strength (in this study, 0.0025) and the region where the concrete strain is more than spalling strain (in this study, 0.006), should be investigated. These regions are represented by $L_{cs}$, and $L_{cc}$, respectively. Examination of numerical results shows that; the value of $L_{cc}$ is limited to the value of $L_{cs}$. Therefore, the maximum length of the concrete crushing zone $L_{cs}$ , is considered (Zhao et al., 2011). To investigate the rebar yielding zone and concrete crushing zone, the rebar and concrete strain distribution curves of specimens were extracted from the ABAQUS software (Fig. 12 and Fig. 13). It should be noted that due to the symmetry of the simply supported beams, the results are presented for half the beams. According to the results, it can be stated that increasing the depth of the simply supported beams increases the length of the rebar yielding zone and the concrete crushing zone. Fig. 14 depicts the equivalent plastic strain contour of specimens. It has been found that in normal beams the concrete crushing zone is focused on the middle span, but in simply supported deep beams the concrete crushing zone spreads along the compression trajectory from the loading place toward the support. This is due to the force transferring mechanism of deep beams. The main force transferring mechanism of deep beams is tied arch action, which can be described by the generation of a compression force in the web that in turn yields to a tension force in the perpendicular direction. In the STM model, the reinforced concrete element is idealized as an equivalent truss and analyzed for applied loads. The compression zones are represented as struts, while tension zones are converted into ties, which are in turn connected at the nodes to form a truss (Zhao et al., 2012). Different types of struts are shown in Fig 15. As can be seen from results in deep beams under concentrated load because of the creation of the bottle-shaped strut, the concrete

damage zone is clearer and more intense compared with deep beams under distributed load.

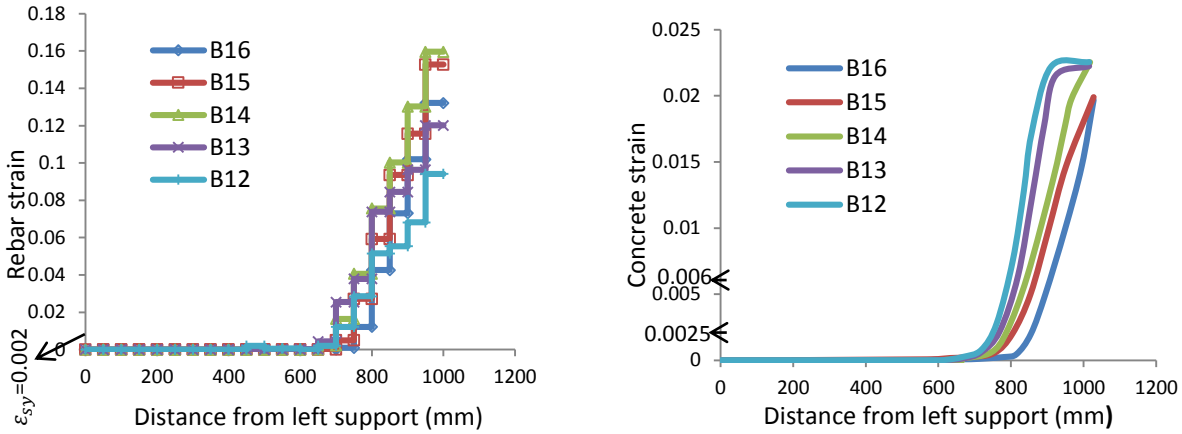


(a) (b)

**Fig. 12**. Beams under concentrated loading. (a) Rebar yielding length, (b) Concrete crushing length.

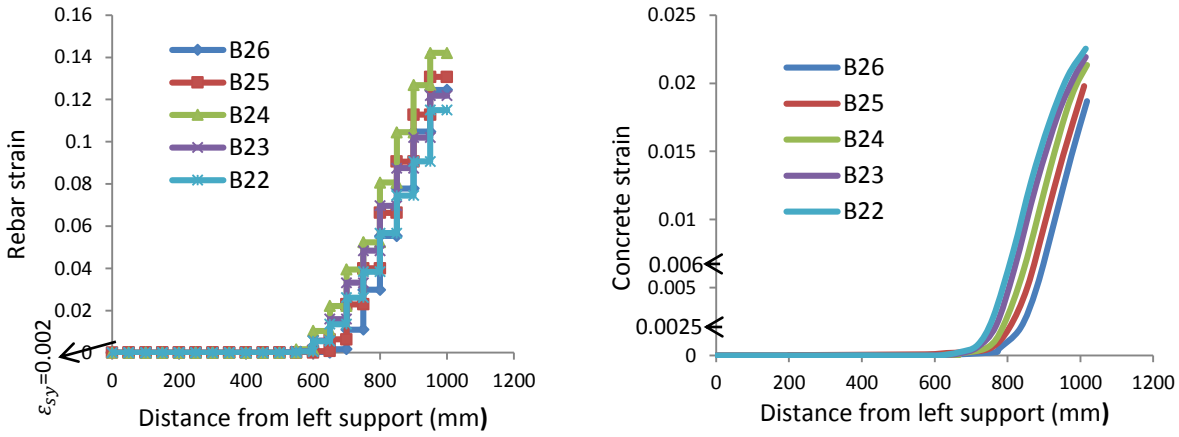


(a) (b)

**Fig. 13**. Beams under distributed loading. (a) Rebar yielding length, (b) Concrete crushing length

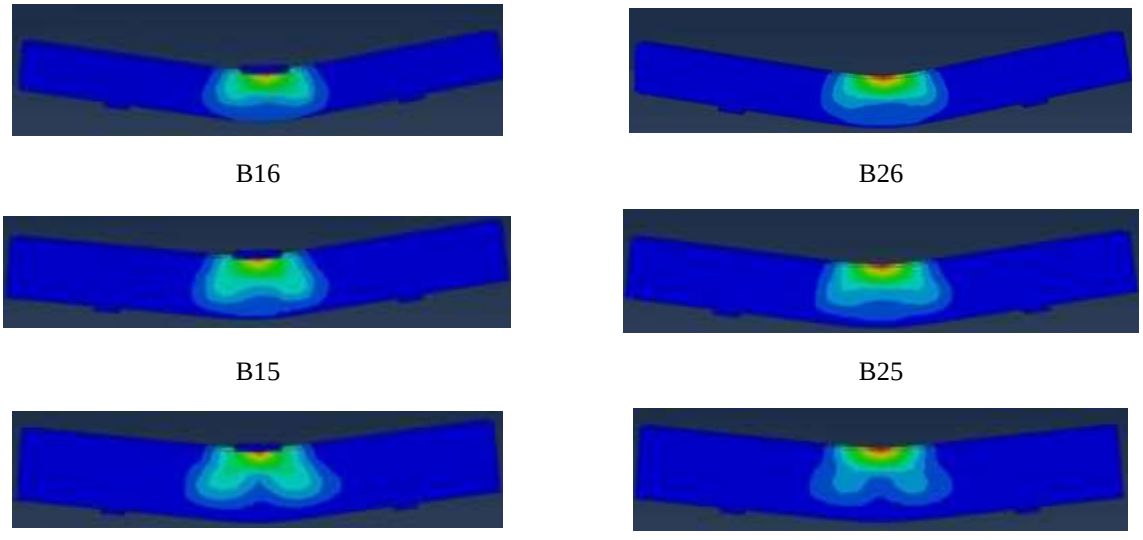

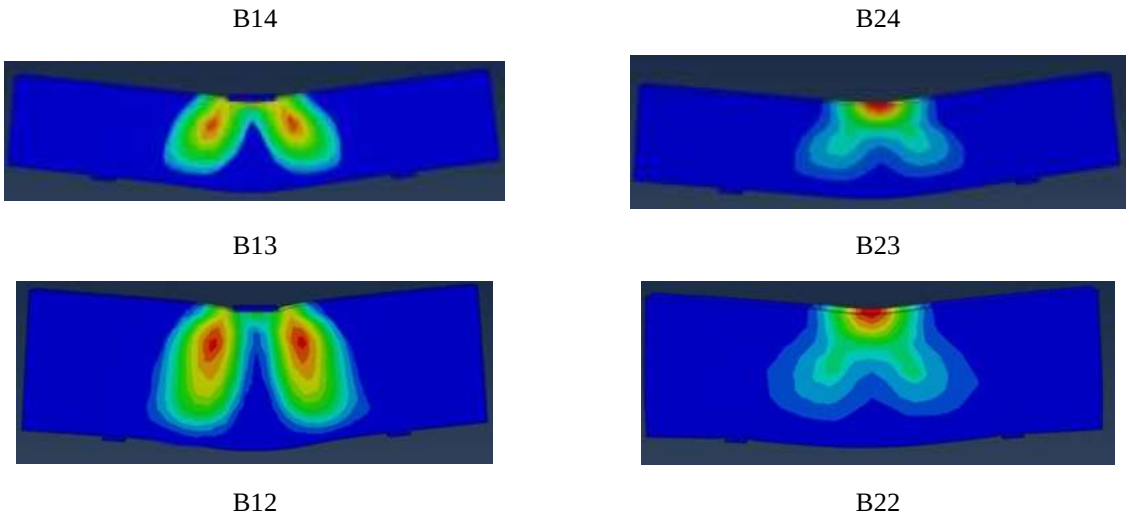


**Fig. 14.** Equivalent plastic strain (PEEQ) contour of the beams

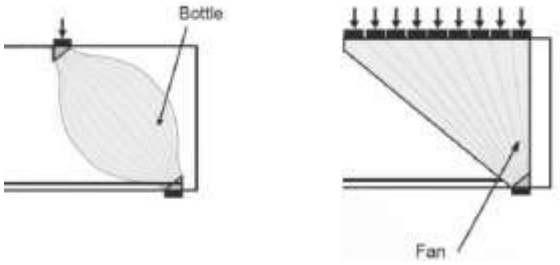


**Fig. 15**. Different types of struts

It can be seen from Table 3 that the length of the rebar yielding zone is the highest level of plastic hinge zones for all specimens. The process of increasing the length of the rebar yielding zone becomes slower with increasing beam depth, in the other word in simply supported deep beams increasing depth of the beam has less effect on rebar yielding length compared with normal beams. As can be seen from the results, the rebar yielding zone length increases about 15%-20% as the loading type is changed from the centrally concentrated load to uniformly distributed load, but the concrete crushing zone length in the compression surface of the beam is the same for beams under concentrated and distributed loads. The length of the rebar yielding zone and concrete crushing zone, for beams with variable drift ratios, were evaluated (Table4). Fig. 16 illustrates the obtained curves in beam B16 as a typical case. Results show that plastic hinge regions extend as the displacement (Drift ratio) of the beams increases. Analytical results were compared with empirical equations presented in Table1; it was observed that the numerical results of normal beams are closer to the Paulay and Priestly model. Whereas empirical predictions by baker and Corley, which Consider the effect of the span-to-depth ratio of the beam, are more accurate for predicting the length of the plastic hinge of deep beams.

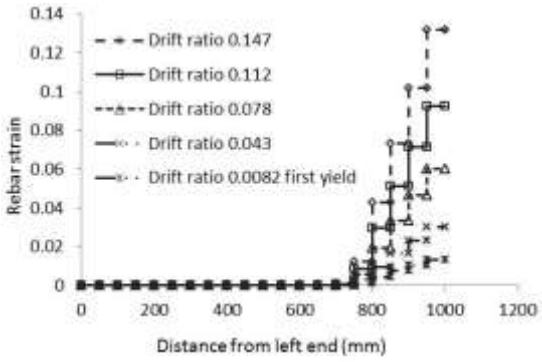


(a)

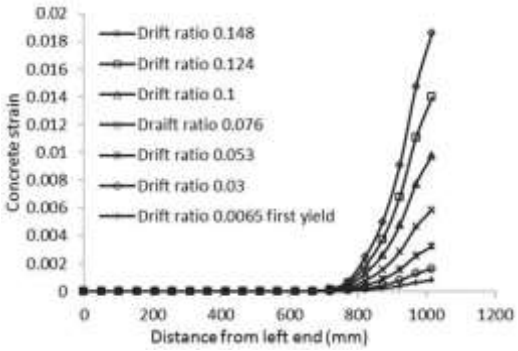


(b)

**Fig. 16**. Distribution of Rebar and Concrete strains for one sample of beams, B16: (a) Rebar strain, (b) Concrete strain

**Table 3**. Numerical results obtained for the beams

| Beam ID | Deflection at yield $\Delta_y$(mm) | Deflection at ultimate $\Delta_u$(mm) | Load at yield $F_y$(KN) | Load at ultimate $F_u$(KN) | Length of concrete crushing $L_{cs}$(mm) | Length of rebar yielding $L_{sy}$(mm) | $\frac{L_{cs}}{d}$ | $\frac{L_{sy}}{d}$ |
|---|---|---|---|---|---|---|---|---|
| B16 | 5.03 | 90.05 | 140.56 | 171.25 | 150 | 250 | 0.58 | 1.47 |
| B15 | 3.80 | 80.21 | 178.93 | 223.01 | 200 | 300 | 0.71 | 1.42 |
| B14 | 3.25 | 75.13 | 260.71 | 330.24 | 250 | 325 | 0.92 | 1.29 |
| B13 | 3.02 | 45.70 | 367.02 | 469.05 | 275 | 340 | 0.81 | 0.94 |
| B12 | 2.60 | 30.21 | 613.50 | 764.23 | 300 | 350 | 0.5 | 0.58 |
| B26 | 5.14 | 100 | 236.94 | 275.62 | 1q50 | 300 | 0.88 | 1.76 |
| B25 | 4.17 | 88.31 | 305.91 | 370.49 | 200 | 350 | 0.95 | 1.66 |
| B24 | 3.52 | 80.62 | 448.67 | 551.43 | 250 | 375 | 0.92 | 1.48 |
| B23 | 3.12 | 50.43 | 651.87 | 784.33 | 275 | 390 | 0.81 | 1.08 |
| B22 | 2.87 | 35.02 | 1075.41 | 1337.52 | 300 | 400 | 0.5 | 0.66 |

**Table 4**. Variation of plastic hinge regions ($L_{sy}$. $L_{cs}$) with increasing Drift ratio

| Beam ID | Drift ratio | Lsy | Lcs | Drift ratio | Lsy | Lcs | Drift ratio | Lsy | Lcs | Drift ratio | Lsy | Lcs | Drift ratio | Lsy | Lcs |
|---|---|---|---|---|---|---|---|---|---|---|---|---|---|---|---|
| B16 | 0.008 | 100 | 50 | 0.04 | 125 | 50 | 0.078 | 150 | 75 | 0.1 | 200 | 100 | 0.14 | 250 | 150 |
| B15 | 0.006 | 100 | 50 | 0.03 | 150 | 75 | 0.065 | 200 | 100 | 0.1 | 250 | 125 | 0.13 | 300 | 200 |
| B14 | 0.0053 | 100 | 100 | 0.035 | 175 | 150 | 0.063 | 225 | 200 | 0.09 | 300 | 225 | 0.123 | 325 | 250 |
| B13 | 0.005 | 150 | 125 | 0.023 | 200 | 150 | 0.04 | 250 | 225 | 0.06 | 300 | 275 | 0.075 | 340 | 275 |
| B12 | 0.004 | 150 | 125 | 0.015 | 200 | 150 | 0.027 | 250 | 200 | 0.36 | 300 | 250 | 0.05 | 350 | 300 |
| B26 | 0.0084 | 75 | 50 | 0.045 | 125 | 75 | 0.086 | 200 | 100 | 0.125 | 225 | 125 | 0.164 | 300 | 150 |
| B25 | 0.007 | 100 | 50 | 0.04 | 150 | 100 | 0.075 | 225 | 125 | 0.11 | 275 | 150 | 0.145 | 350 | 200 |
| B24 | 0.0057 | 150 | 75 | 0.035 | 250 | 125 | 0.07 | 300 | 200 | 0.1 | 350 | 225 | 0.13 | 375 | 250 |
| B23 | 0.005 | 150 | 100 | 0.025 | 225 | 150 | 0.046 | 300 | 200 | 0.063 | 375 | 250 | 0.084 | 390 | 275 |
| B22 | 0.0035 | 200 | 150 | 0.018 | 250 | 200 | 0.028 | 300 | 225 | 0.045 | 350 | 275 | 0.06 | 400 | 300 |

## 5. Conclusions

In this work, the plastic hinge regions of deep beams were investigated and compared with normal beams. Based on the analytical results, conclusions can be summarized as:

- The strain distribution across the depth of deep beams is not a straight line and curvature at different heights of the deep beam does not have the same trend as that in a normal beam. Therefore, the curvature localization zone is not suitable for the prediction of plastic hinge length in deep beams.
- In Normal beams the concrete crushing zone is focused on the middle span, but in deep beams by creating a compression strut between loading place and support, the concrete crushing zone spreads along the compression trajectory. In deep beams under concentrated load because of the creation of the bottle-shaped strut from the loading place toward support, the concrete damage zone is more intense compared with deep beams under distributed load.
- The value of the rebar yielding zone on one side of the critical section for simply supported beams does not exceed twice the effective depth in the studied beams in this work. In simply supported deep beams increasing depth of the beam has less effect on rebar yielding length compared with Normal beams.
- The loading type affects the plastic hinge length. The rebar yielding length increases about 15%-20% as the loading type is changed from the centrally concentered load to uniformly distributed load in simply supported beams.
- The plastic hinge regions extend as the drift ratio of the beam increases. Among the empirical models that are used for the prediction of plastic hinge length in Normal beams, the equations that take into account

the effect of the span-to-depth ratio of the beam, are most accurate for deep beams.

## References


Abdel-Fattah B, Wight JK, "Study of moving beam plastic hinging zones for earthquake-resistant design of reinforced concrete buildings", Structural Journal, 1987, 84, 31-39.

Adinkrah-Appiah K, Adom-Asamoah M, "Characterization and Shear Strength Prediction of Reinforced Concrete Deep Beams-A Review, 2016.

Aguilar G, Matamoros AB, Parra-Montesinos G, Ramírez JA, Wight JK, "Experimental evaluation of design procedures for shear strength of deep reinfoced concrete beams", American Concrete Institute, 2002.

Abdel-Fattah B, Wight JK, "Study of moving beam plastic hinging zones for earthquake-resistant design of reinforced concrete buildings", Structural Journal, 1987, 84, 31-39. https://doi.org/10.14359/2767.

Adinkrah-Appiah K, Adom-Asamoah M, "Characterization and Shear Strength Prediction of Reinforced Concrete Deep Beams-A Review", International Journal of Science And Research, 2016, 5 (3), 1789-1798.

Aguilar G, Matamoros AB, Parra-Montesinos G, Ramírez JA, Wight JK, "Experimental evaluation of design procedures for shear strength of deep reinfoced concrete beams", American Concrete Institute, 2002.

Arabzadeh A, Aghayari R, Rahai A.R, "Investigation of experimental and analytical shear strength of reinforced concrete deep beams", International Journal of Civil Engineering, 2011, 207-214.

Baker AL, "The ultimate load theory applied to the design of reinforced & prestressed concrete frames", Concrete Publ. Lmd, 1956.

Chen H, Yi WJ, Hwang HJ, "Cracking strut-and-tie model for shear strength evaluation of reinforced concrete deep beams", Engineering Structures, 2018, 163, 396-408. https://doi.org/10.1016/j.engstruct.2018.02.077.

ACI committee 318, "Building code requirements for structural concrete", 2014.

Coleman J, Spacone E, "Localization issues in force-based frame elements", Journal of Structural Engineering, 2001, 127, 1257-1265. https://doi.org/10.1061/(ASCE)0733-9445(2001)127:11(1257)

Corley WG, "Rotational capacity of reinforced concrete beams", Journal of the Structural Division, 1966, 92, 121-146. https://doi.org/10.1061/JSDEAG.0001504.

Demir A, Caglar N, Ozturk H, "Parameters affecting diagonal cracking behavior of reinforced concrete deep beams", Engineering Structures, 2019, 184, 217-231. https://doi.org/10.1016/j.engstruct.2019.01.090

Elmenshawi A, Brown T, El-Metwally S, "Plastic hinge length considering shear reversal in reinforced concrete elements", Journal of Earthquake Engineering, 2012. https://doi.org/10.1080/13632469.2011.597485

Ghazi-Nader D, Aghayari R, "Plastic hinge region in simply supported RC deep beams", Third International Conference and 7th National Conference on Civil Engineering Materials and Structures, Bu-Ali Sina University, Iran, 2018.

Hussein G, Sayed SH, Nasr NE, Mostafa AM, "Effect of loading and supporting area on shear strength and size effect of concrete deep beams", Ain Shams Engineering Journal, 2018, 9, 2823-2831. https://doi.org/10.1016/j.asej.2017.11.002

Ibrahim MA, El Thakeb A, Mostfa AA, Kottb HA, "Proposed formula for design of deep beams with shear openings", HBRC Journal, 2018, 14, 450-465. https://doi.org/10.1016/j.hbrcj.2018.06.001.

Kheyr AA, Naderpour H, "Plastic hinge rotation capacity of reinforced concrete beams", 2007.

Legeron F, Paultre P, "Behavior of high-strength concrete columns under cyclic flexure and constant axial load", Structural Journal, 2000, 97, 591-601. https://doi.org/10.14359/7425

López AM, Sosa PF, Senach JL, Prada MÁ, "Influence of the plastic hinge rotations on shear strength in continuous reinforced concrete beams with shear reinforcement", Engineering Structures, 2020, 207, 110242. https://doi.org/10.1016/j.engstruct.2020.110242

Ma C, Xie C, Tuohuti A, Duan Y, "Analysis of influencing factors on shear behavior of the reinforced concrete deep beams", Journal of Building Engineering, 2022, 45, 103383. https://doi.org/10.1016/j.jobe.2021.103383.

Manual AU. version 6.8: Providence: Hibbit. Karlsson and Sorenson, 2008.

Mattock AH, "Discussion of Rotation Capacity of Reinforced Concrete Beams", Journal of Structual Division, 1967, 93, 519-522. https://doi.org/10.1061/JSDEAG.0001678.

Mohamed AR, Shoukry MS, Saeed JM, "Prediction of the behavior of reinforced concrete deep beams with web openings using the finite element method", Alexandria Engineering Journal, 2014, 53, 329-339. https://doi.org/10.1016/j.aej.2014.03.001

Mohamed N, Farghaly AS, Benmokrane B, Neale KW, "Flexure and shear deformation of GFRP-reinforced shear walls", Journal of Composites for Construction, 2014, 18, 04013044.

https://doi.org/10.1061/(ASCE)CC.1943-5614.0000444

Niranjan BR, Patil SS, "Analysis of RC deep beam by finite element method", International Journal of Modern Engineering Research (IJMER), 2012, 2, 4664-4667.

Panagiotakos TB, Fardis MN, "Deformations of reinforced concrete members at yielding and ultimate", Structural Journal, 2001, 98, 135-148. https://doi.org/10.14359/10181

Park R, Paulay T, "Reinforced concrete structures", John Wiley & Sons, 1991.

Paulay T, Priestley MN, "Seismic design of reinforced concrete and masonry buildings", 1992.

Pereira N, Romão X, "Damage localization length in RC frame components: Mechanical analysis and experimental observations", Engineering Structures, 2020, 221, 111026. https://doi.org/10.1016/j.engstruct.2020.111026

Pokhrel M, Bandelt MJ, "Plastic hinge behavior and rotation capacity in reinforced ductile concrete flexural members", Engineering Structures, 2019, 200, 109699. https://doi.org/10.1016/j.engstruct.2019.109699

Roy NC, Brena SF, "Behavior of deep beams with short longitudinal bar anchorages", ACI Structural Journal, 2008, 105, 460.

Herbert A, Sawyer JR, "Design of concrete frames for two failure stages", Special Publication, 1964, 12, 405-437. https://doi.org/10.14359/16726

Schlappal T, Kalliauer J, Vill M, Mang HA, Eberhardsteiner J, Pichler BL, "Ultimate limits of reinforced concrete hinges", Engineering Structures, 2020, 224, 110889. https://doi.org/10.1016/j.engstruct.2020.110889

Wang GL, Meng SP, "Modified strut-and-tie model for prestressed concrete deep beams", Engineering Structures, 2008, 30, 3489-3496. https://doi.org/10.1016/j.engstruct.2008.05.020

Yang KH, Chung HS, Lee ET, Eun HC, "Shear characteristics of high-strength concrete deep beams without shear reinforcements", Engineering structures, 2003, 25**,** 1343-1352. https://doi.org/10.1016/S0141-0296(03)00110-X

Zhao XM, Wu YF, Leung AY, "Analyses of plastic hinge regions in reinforced concrete beams under monotonic loading", Engineering Structures, 2012, 34, 466-482. https://doi.org/10.1016/j.engstruct.2011.10.016

Zhao X, Wu YF, Leung AY, Lam HF, "Plastic hinge length in reinforced concrete flexural members", Procedia Engineering, 2011, 14, 1266-1274. https://doi.org/10.1016/j.proeng.2011.07.159.